Laboratory study of displacements in a geogrid reinforced soil model under lateral earth pressures

Lissette Ruiz-Tagle, CSP-DSI, Chile, lruiz-tagle@csp-dsi.cl
Felipe Villalobos, Catholic University of Concepción, Chile, avillalobos@ucsc.cl

ABSTRACT

An experimental and numerical study is presented related to displacements and rotations of soil particles without and with geogrid reinforcement under the application of active lateral earth pressures. To this end, the measurement technique PIV has been used, with which digital images are processed to obtain displacement and rotation fields. The experimental earth pressure equipment has a transparent window which allows the recording of soil particle movements. The process and analysis of the measured soil particle movements allow the determination of yielded and not yielded soil areas. In this form, the position and geometry of the failure surface was determined and compared with the defined by plasticity theory of active Rankine states. This comparison is only possible for the case without geogrids since the presence of geogrids changes significantly the zone of soil yielding. Geogrids can reduce up to twice the volume of yielded soil due to the active lateral earth pressure. This conclusion related to the soil deformation is found to be in direct relation with the active lateral earth pressure reduction when geogrids are used as reinforced elements. In addition, a numerical analysis using the computational program Plaxis was performed to estimate horizontal displacements. The numerical results estimate reasonably well the horizontal displacements measured in terms of the general shape of the soil yielding area. However, they do not reproduce in detail the geometry of the failure surface.

1. INTRODUCTION

The contribution of geogrids to the improvement of strength capacity and deformation reduction of foundation soils and artificial fills has been recognised within Geotechnical Engineering (*e.g.* Giroud 1986; Koerner 1986; Müller-Rochholz 2008). Moreover, construction methods can be more attractive economically, versatile in installation and less time consuming than traditional gravity or cantilever retaining walls. They have a good seismic response, for instance, no major damage has been found during the 2010 Chile earthquake of magnitude 8.8. Additionally, it has been found that geogrid reinforced soils can have a lesser carbon footprint than traditional retaining wall structures (O'Riordan *et al.,* 2011).

The study of active lateral earth pressure of compacted and reinforced fills against retaining structures is based mainly on plasticity theory, applying the Rankine stress states (Jones 1984, 1996). However, results of horizontal stresses measured by Berg *et al.* (1986) in retaining walls of 4.65 m y 6 m high with geogrid reinforced soil, were lower than that determined by the plasticity theory. Furthermore, the use of geogrids can significantly change the linear earth pressure distribution with depth. Differences with the linear distribution theory have also been shown by Pachomow *et al.* (2007), who have presented results from lateral earth pressure tests carried out on a 3.5 m high wall with a geogrid reinforced soil, comparing the results with that collected from a large database. These differences have been reflected, in part, in an updated version of the EBGEO (2009) recommendations, where the lateral earth pressure acting on a geogrid reinforced wall is lower than that proposed in the previous 1997 version.

There is scarce information available in the technical literature about experimental results of displacements and rotations of soil particles in geogrid reinforced walls under constant overburden σ. The little information available has been obtained numerically by means of the Method of Finite Element MFE (*e.g.* Pachomow *et al.* 2007). For that reason this experimental work focuses mainly on the analysis of the displacement variation of the soil retained behind a vertical wall. To this end, the image treatment technique PIV has been used. Finally, numerical analyses are carried out using the computing program Plaxis.

1.1. Experimental set-up

The equipment used and shown in Figure 1, has been designed and built by Ruiken *et al.* (2010a, 2010b, 2011). Additional information about the experimental set-up, Marienberg sand preparation and geogrid

characteristics can be found in Ruiz-Tagle and Villalobos (2011). They analyse the stress distribution results for the same tests, but they do not consider displacement and rotations as presented in this article.

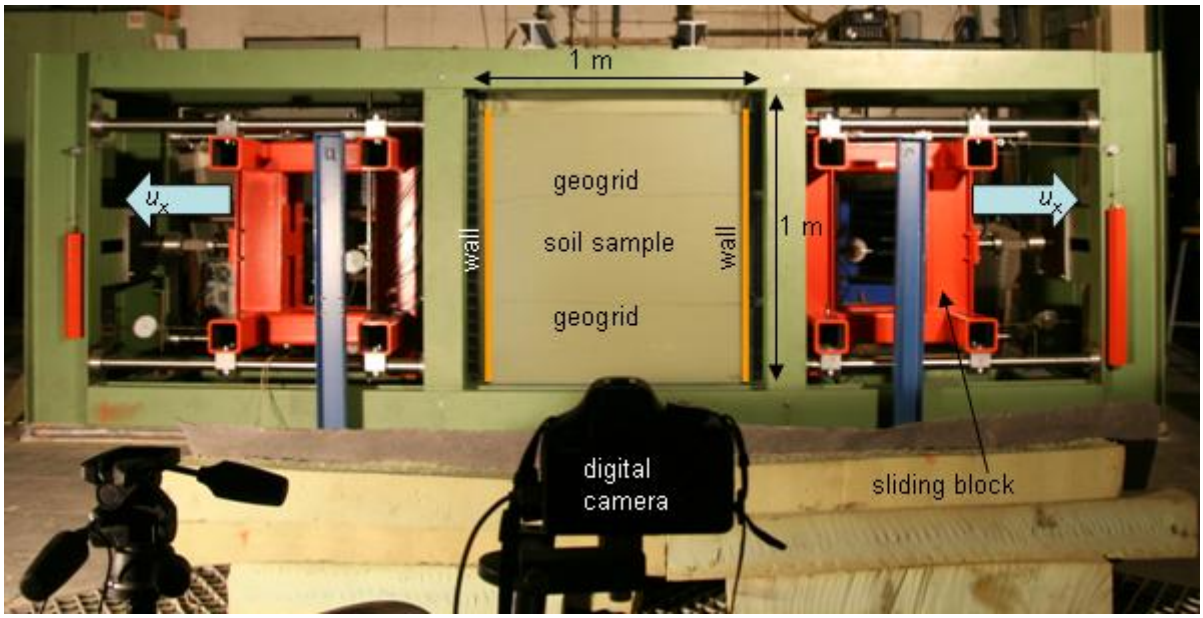

Figure 1: Experimental equipment for lateral earth pressure tests, showing the sample with two geogrids highlighted with black sand next to the glass window and the location of two digital cameras for PIV displacement analyses

The soil sample dimensions are 1 m high, 1 m long and 0.45 m wide (see Figure 1). There are two independent walls at each side which can be displaced manually by means of a block sliding along four horizontal bars. The active lateral earth pressure is obtained by the application of a block displacement u_x as shown in Figure 1. This set-up can model a scaled wall, but it can be also considered as a particular part of a wall as shown in a square in Figure 2.

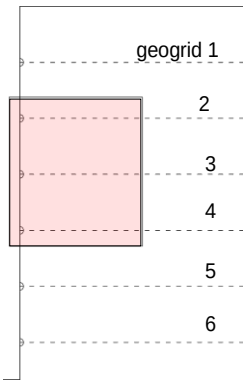

Figure 2: Retaining structure prototype with geogrid reinforced soil, showing the part studied in the laboratory

2. DETERMINATION OF THE SOIL DISPLACEMENTS

An optic method was used to study the soil displacement which is reinforced with geogrids. This method, known as PIV (Particle Image Velocimetry), allows the determination of movements and rotations of soil particles on a visible plane, usually behind a glass or a transparent material. A digital camera is required to capture every certain time intervals a focused and fixed frame, and in this form the movement of soil grains can be tracked. In this study sand grains move due to the active lateral earth pressure imposed by a sliding block inducing displacements u_x on a retaining wall in sequences of 0.1 mm until to reach a total u_x of 10 or 20 mm. The initial zero displacement allows the determination of the lateral earth pressure at rest. Ruiz-Tagle and Villalobos (2011) report that the active lateral earth pressure is completely developed

for a wall displacement u_x of 0.2 mm in a soil sample without reinforcement. This occurred when the measured horizontal stresses become similar to that calculated with the Rankine theory. Geogrid's positions were possible to observe with the assistance of dark sand, spread along the geogrid next to the window (see Figure 1 y 3). Figure 3 shows a detail of the soil settlement and geogrid distortion on the wall upper part.

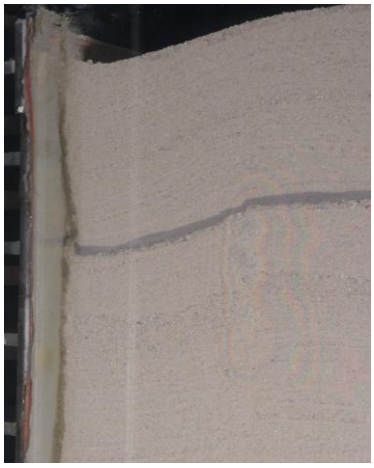

Figure 3: Distortion detail of the geogrid and soil settlement

During the lateral earth pressure tests snapshots were taken to the whole sample and in some cases another camera was used to determine in more detail a particular area. In each test the location of the camera was the same, 0.7 m high from the floor to the objective centre allowed to capture the complete frontal area of the soil sample. Snapshots were taken for each interval of wall horizontal displacement u_x = 0.1 mm. Information about the PIV technique can be read in White *et al.* (2003) and White and Bolton (2004).

2.1 Results in soil without reinforcement

As a first stage in the study of active lateral earth pressure, measurements were performed without geogrid reinforcement. Figure 4 shows the displacement field and rotation variations of soil particles obtained after processing the PIV data for four levels of wall horizontal displacement u_x = 0, 0.6, 3 and 20 mm. The displacement and rotation fields are interpreted by means of displacement vectors and as clockwise or anticlockwise rotations, representing qualitative and relative parameters as shown by arrows and colours in Figure 4. For a wall displacement u_x = 0.6 mm, a slightly marked zone of soil can be hardly observed in movement. This establishes a difference with Ruiz-Tagle and Villalobos (2011) observation of active pressure development for u_x = 0.2 mm, from the stress distribution results. This difference might be related to the at rest pressure effect, which is higher than the active pressure, but without inducing displacements, *i.e.* it does not affect the displacement measurements.

For $u_x \geq 3$ mm the PIV results allow clear observation of the development of a zone where rotations are higher, defining a boundary or failure surface. According to plasticity theory a failure surface follows a straight line forming with the horizontal an angle $\theta = 45^o + \phi/2$. Since the sand was tested with a relative density of 93%, corresponding to a triaxial angle of friction $\phi_{tx} = 40^o$, results in $\theta = 65^o$. Some little adjustment can be done to correct the fact that a plane strain angle of friction ϕ_{ps} should be used. Thus, using $\phi_{ps} = 46^o$ according to Lee (1966), results in $\theta = 68^o$, still below $\theta = 75^o$, value obtained from the earth pressure test results shown in Figure 4. This means that a plastic equilibrium state or Rankine active state involves a larger area of plastified soil than that measured. It is worth noting that the failure surface tends to be vertical when reaches the upper part. This may be attributed to larger horizontal and vertical displacements (settlement) occurring in the upper part compared with the bottom part of the wall.

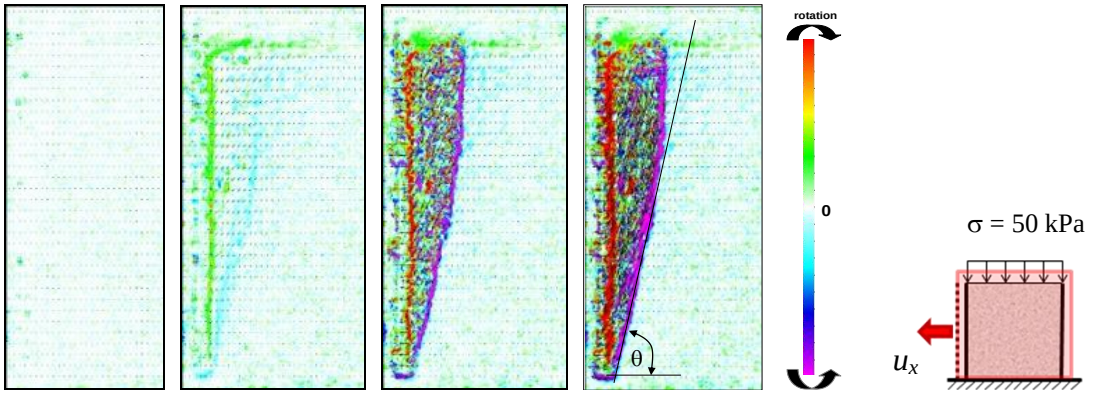

u_x = 0 mm u_x = 0.6 mm u_x = 3 mm u_x = 20 mm

Figure 4: Rotation of soil particles for different wall displacements for an overburden of 50 kPa

2.2 Results in reinforced soil

The following results correspond to displacement and rotation fields of soil particles when geogrids were used as a reinforcement material in the soil behind a wall moved forward to generate an active earth pressure condition. The soil sample was reinforced with one, two, three and four geogrids, respectively. Inside the 1 m high sand sample, one geogrid was located in the middle, two geogrids were located from the top at 0.3 and 0.7 m, three geogrids at 0.2, 0.5 and 0.8 m and four geogrids at 0.1, 0.35, 0.65 and 0.9 m, respectively. Figure 5 shows the displacement field represented by vectors and rotation of particles represented by colours, after the wall has displaced 10 mm. It can be observed that geogrids restrain the failure surface to extend and involve more soil (see the horizontal black arrow on top to compare with the case without geogrid). The boundary between soil with and without movement, *i.e.* the failure surface, adopts a curve shape between geogrids. This change in shape also occurs in the horizontal stress distribution between geogrids as reported by Ruiz-Tagle and Villalobos (2011). They point out that the earth pressure reduction is related to the formation of stress arcs between geogrids. Then, this earth pressure reduction is taken in the form of a tension stress in the opposite direction by the geogrids.

Looking at the vector's directions in Figure 5, it is possible to observe that in general the vertical component predominates over the horizontal component of grain movement. The vertical movement of grains tends to be higher on the sample upper part and the horizontal component relative to the vertical tends to increase in grains next to the wall and closer to the wall base. Moreover, grains located closer to the wall undertake larger relative magnitude of movement. This relative movement of grains reduces with the distance from the wall towards the failure surface. Furthermore, the maximum rotations occur clockwise for soil grains next to the wall (red colour) and anticlockwise for soil grains in the failure surface (pink colour).

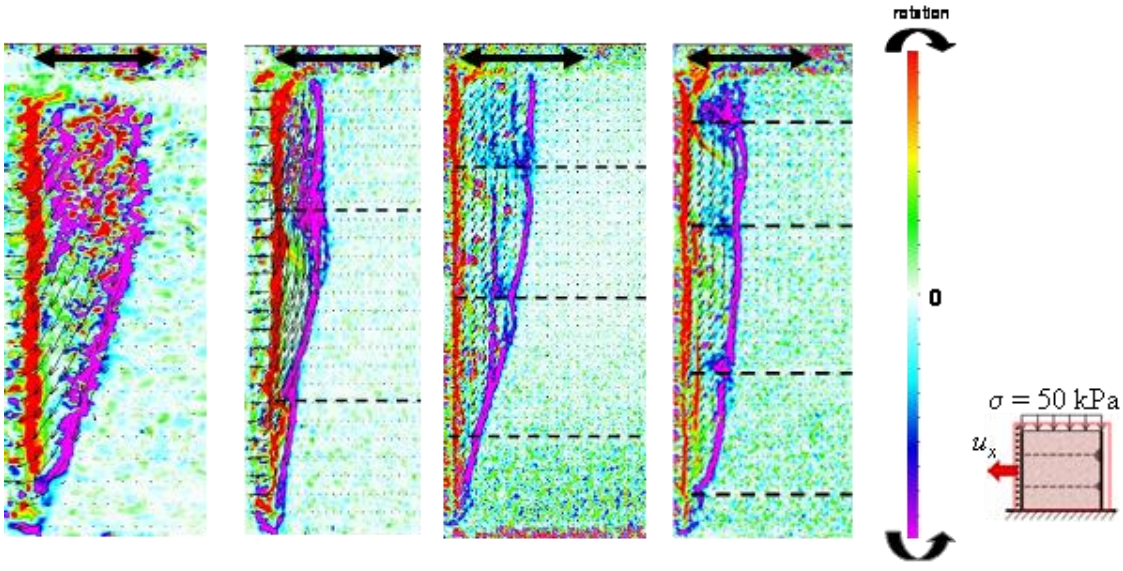

Figure 5: Displacement vectors and particle rotation in colours without and with two, three and four geogrids, overburden σ = 50 kPa and u_x = 10 mm

In Figure 6, a detail of 0.3 m by 0.2 m located next to the wall and on the upper part, compares the cases without and with geogrid for u_x = 10 mm and an overburden σ = 50 kPa. The geogrid distortion due to settlement can be observed in Figure 6a. Horizontal displacement results obtained using the PIV technique with high resolution images (15 megapixels) are shown in Figure 6b for the cases without and with geogrid. The blue colour indicates the absence of displacements and the red colour represents the maximum values of horizontal displacement. These results also reveal that the geogrid reduces considerably the area of the soil yielding (red and yellowish zone). Furthermore, without the geogrid horizontal displacements vary uniformly from left to right (from red to green). Whereas with the geogrid, maximum horizontal displacements concentrate above the geogrid, hence, the gradual and uniform variation disappears.

In terms of displacement vectors, Figure 6c on the left shows the case without geogrid, where a unique and inclined failure surface develops. However, in the case with the upper geogrid (on the right hand side of Figure 6c and in terms of rotations), not only a main vertical failure surface is formed, but also another two almost parallel failure surfaces appear. Moreover, it is possible to observe the development of a failure line between the wall and the geogrid descending in 45º until it touches one of the parallel vertical failure surfaces. Despite the geogrid is not fixed to the wall, shear stresses are transmitted between the geogrid and the soil, which form a soil triangle above and below the failure line in 45º. The triangle above moves downwards, acting as an active wedge pushing the triangle below to the left. This follows observations pointed out by Ruiken *et al.* (2010b).

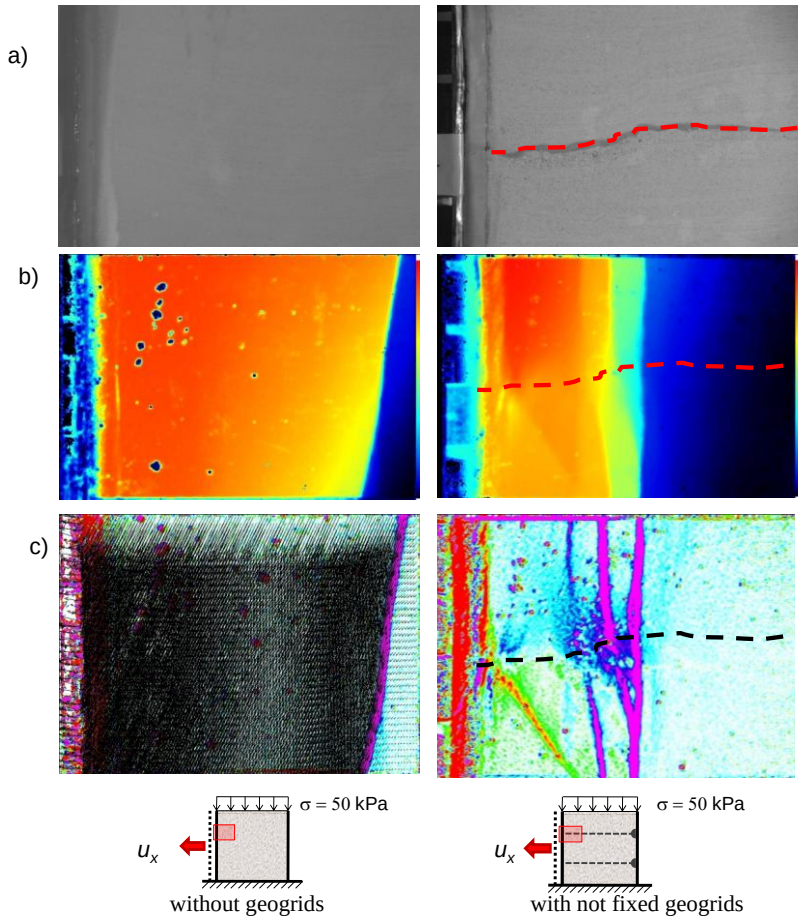

Figure 6: Details of the soil next and on top of the wall for u_x = 10 mm and σ = 50 kPa, a) distorted soil, b) horizontal displacements obtained with PIV and c) displacement vectors and particle rotation

2.3 Numerical analysis

The bi-dimensional finite element computing program Plaxis was used to study soil deformation. Modelling was performed for a plane strain condition with 15 nodes per element. It was considered that a medium mesh density with 98% accuracy was sufficient for the calculations. Fine and very fine meshes need higher computational resources and time to achieve a little accuracy increment. Boundary conditions were studied in order to simulate earth pressure laboratory tests. Soil-structure interaction effects were

taken into account, for the development of appropriate movements in the contact between the wall and the soil. However, in a finite element analysis, the use of continuous elements with displacement compatibility might not allow these movements in the soil. Consequently, when using the FEM a nodal compatibility condition has to be implemented to achieve coordinated movements among adjacent elements, *i.e.* without overlapping. To implement nodal compatibility Plaxis has the *interface* option for elements used in the modelling of contact surfaces, in this case between the wall and the soil. In this form, it was possible to modify the constitutive behaviour of contact surfaces (friction among different materials), and relative movements can be possible as well (sliding and separation).

Figure 7 shows a modelling result without using *interface*. Despite the active earth pressure applied, soil elements next to the wall do not settle, which is the opposite of that observed in the experiments (see Figure 3). This is due to the boundary conditions imposed in the modelling, *i.e.* a wall with too much friction does not allow the soil to slide and settle.

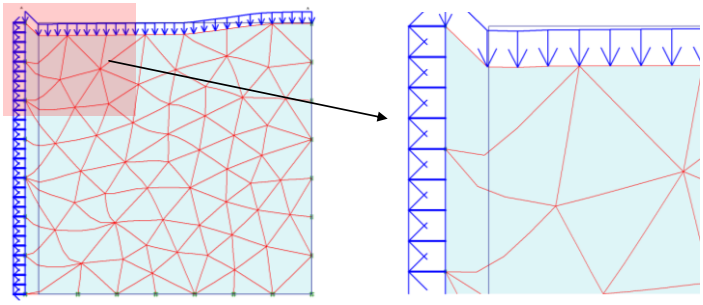

Figure 7: Deformed mesh without geogrid and not using interface

When a value of *interface* R_{inter} = 1 was used, the adherence effect between the soil and the wall disappear. However, this is not correct because a gap opens between the wall and the soil as shown in Figure 8, which does not reproduce the experimental results. Finally, in the computational simulations a value of R_{inter} = 0.3 was used in view of the better representation of the expermiental interface angle of friction wall-soil of 2.6º. This value was also found to represent well the experimentally measured settlements. R_{inter} values lower than 0.3 are not recommended because the soil overlaps the wall, which is not real, resulting in deformation incompatibility.

The soil geotechnical parameter values used in the modelling are a dry unit weight γ_d = 17.3 kN/m^3 and an angle of internal friction ϕ_{tx} = 40º. An elasticity modulus E = 10^5 kPa and a Poisson's ratio of 0.25 were assumed. The triaxial angle of internal friction was changed to 46º to take account of the plane strain condition according to Lee (1970). The geogrid stiffness value adopted was EA = 2100 kN/m.

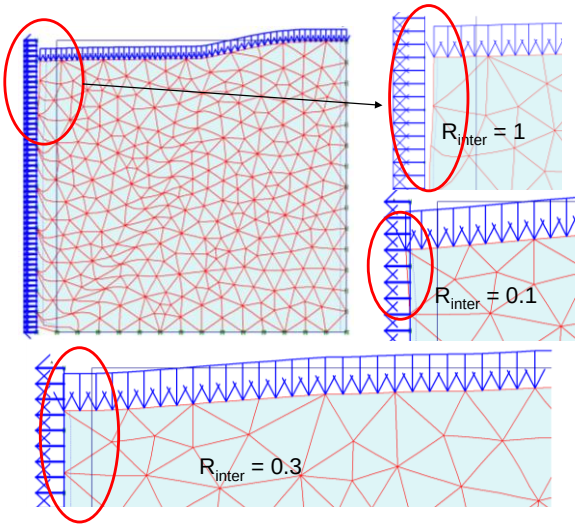

Figure 8: Deformed mesh for non reinforced soil, showing the boundary effect in the contact wall-soil in the upper part using interface R_{inter} = 1, 0.3 and 0.1

Figure 9a shows horizontal displacement results for the case without geogrids and Figure 9b shows the results for the case with two geogrids. It can be observed that the numerical results are able to simulate

the area reduction of soil yielding owing to the geogrid presence when active earth pressure is applied. Displacements arcs are also formed next to wall and between geogrids as observed in the experiments. When comparing Figure 9 with Figures 5 and 6 it can be noted that the numerical simulations are however not able to reproduce the steep slope of the failure surface at the upper part for both cases, without and with geogrids. This difference is probably due to small wall bending on the upper part, *i.e.* wall flexibility. Further research is needed to model numerically displacements and rotations caused by active earth pressure considering wall stiffness.

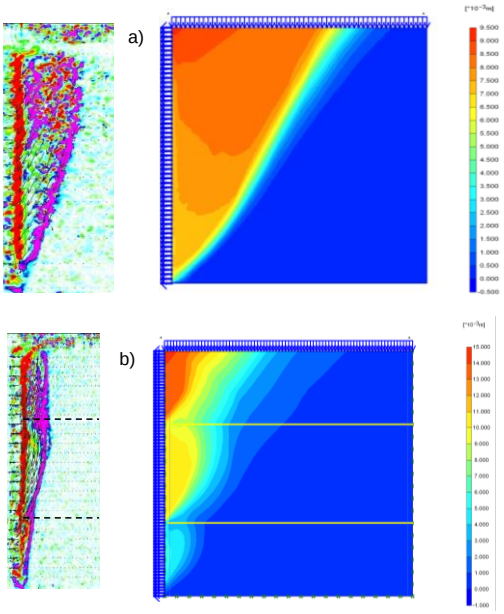

Figure 9: Soil horizontal displacements for σ = 50 kPa and u_x = 10 mm, a) without geogrid and b) with two geogrids (results from Figures 5 and 6 are shown for comparison)

3. CONCLUSIONS

Experimental results of soil particle displacements and rotations behind a retaining wall have been presented and analysed. This was possible by using the PIV technique which allows the definition of soil particle displacement and rotation fields. Analyses of relative displacements and rotations were performed qualitatively by means of displacement vectors and rotation directions, *i.e.* relative magnitudes were obtained without engineering units.

It can be concluded that the area of soil yielding is reduced significantly when geogrids are used. This reduction can reach up to half of the soil volume compared with the case without geogrid. This can explain the reduction of lateral earth pressure measured in the same equipment and reported by Ruiken *et al.* (2011) and Ruiz-Tagle and Villalobos (2011). This pressure reduction is transferred to the geogrids as a tension stress in the opposite direction. Thus, less lateral earth pressure is applied to the retaining structure because the volume of soil yielding is reduced.

A numerical analysis has also been presented using the computing program Plaxis. Initial numerical results are in a general agreement with the experimental results, in terms of the measured horizontal displacements without and with geogrids. However, there are differences related to the shape of the yielding zones. For instance, in the numerical results the yielding zone is wider and the slope of the failure surface on the upper part is much gentler than the almost vertical slope measured in the experiments. Further research is needed to improve numerical analysis.

4. ACKNOWLEDGEMENTS

The work presented in this paper was supported by the German Academic Interchange Service DAAD and the Catholic University of Concepción. The first author is grateful to the advice and supervision of Dipl.-Ing. Axel Ruiken and also appreciates the assistance of the Geotechnical Laboratory staff of the University RWTH-Aachen.

REFERENCES

Berg, R.R., Bonaparte, R., Anderson, R.P. and Chouery, V.E. (1986). Design, construction and performance of two geogrid reinforced soil retaining walls. Proceedings of the Third International Conference on Geotextiles, Vienna Austria, Vol. 2, 401-406

EBGEO (2009). Empfehlungen für den Entwurf und die Berechnung von Erdkörpern mit Bewehrungen aus Geokunststoffen. Deutsche Gesellschaft für Geotechnik

Giroud, J.-P. (1986). From geotextiles to geosynthetics: a revolution in Geotechnical Engineering. Proceedings of the Third International Conference on Geotextiles, Vienna Austria, Vol. 1, 1-18

Jones, C.J.F.P. (1996). Earth reinforcement and soil structures. Thomas Telford

Jones, C.J.F.P. (1984). Design and construction methods. Symposium on Polymer Grid Reinforcement in Civil Engineering. ICE London

Koerner, R.M. (1986). Designing with Geosynthetics. Prentice-Hall

Lee, K. L. (1970). Comparison of plane strain and triaxial test on sand. Journal of the Soil Mechanics and Foundation Division ASCE 96, No. SM3, 901-923

Müller-Rochholz, J. (2008). Geokunststoffe im Erd- und Verkehrswegebau. Werner Verlag
O'Riordan, N., Nicholson, D., Hughes, L. and Phear, A. (2011). Examining the carbon footprint and reducing the environmental impact of slope engineering options. Ground Engineering 44, No 2, 28-30

Pachomow, D., Vollmert, L. und Herold, A. (2007). Der Ansatz des horizontalen Erddrucks auf die Front von KBE-Kronstruktionen. J. Geotechnik Sonderheft, 129-136

Ruiken, A., Ziegler, M., Vollmert, L. and Höhny, I. (2011). Investigation of the compounded behavior of geogrid reinforced soil. Submitted to the Fifteenth European Conference on Soil Mechanics and Geotechnical Engineering, Athens

Ruiken, A., Ziegler, M., Vollmert, L. and Duzic, I. (2010a). Recent findings about the confining effect of geogrids from large scale laboratory testing. 9th International Conference on Geosynthetics, Guarujá, Brazil

Ruiken, A., Ziegler, M., Ehrenberg, H. and Höhny, S. (2010b). Determination of the soil confining effect of geogrids. XIVth Danube-European Conference on Geotechnical Engineering, Bratislava, Slowak Republic

Ruiz-Tagle, L. and Villalobos, F.A. (2011). Experimental study of the lateral earth pressure on retaining structures in soils reinforced with geogrids. Submitted to Revista Ingeniería de Construcción

White, D. J., Take, W.A. and Bolton, M.D. (2003). Soil deformation measurement using particle image velocimetry (PIV) and photogrammetry. Géotechnique 53, No. 7, 619-631

White, D. J. and Bolton, M.D. (2004). Displacement and strain paths during plane-strain model pile installation in sand. Géotechnique 54, No. 6, 375-397